

GENERATION AND DISSIPATION OF DYNAMIC PORE WATER PRESSURES  
IN GRAVEL SHELL EMBANKMENT DAMS BY FINITE ELEMENT METHOD

Carlos A. Prato

Departamento de Estructuras, Facultad de Ciencias Exactas, Físicas y Naturales. Universidad Nacional de Córdoba, Argentina.

Víctor H. Ferrero

Consejo de Investigaciones Científicas y Tecnológicas de la Provincia de Córdoba (CONICOR), Argentina.

RESUMEN

Las presiones de poro producidas en presas de espaldones de gravas por acciones sísmicas son calculadas por un procedimiento desacoplado de dos pasos. En el Paso I, se determina las tensiones estáticas y dinámicas en el cuerpo de la presa con modelos de elementos finitos incorporando el comportamiento no lineal de los materiales. En el Paso II se determina las presiones de poros en función de las tensiones obtenidas en I, y de los resultados de ensayos cíclicos triaxiales no drenados. Finalmente se estudia la disipación de presiones de poros durante el terremoto mediante una solución numérica de la ecuación de la difusión. Un ejemplo numérico ilustra la incidencia del proceso de difusión de las presiones neutras en los valores de los coeficientes de seguridad al deslizamiento después de finalizado el sismo.

ABSTRACT

Dynamic pore water pressures induced on gravel-shell embankment dams by earthquake motions are studied by means of a computational scheme based on a two-step decoupled procedure. In Step I, a static and dynamic stress analysis is performed with standard finite element techniques accounting for non linear soil properties. In Step II, pore water pressure increases are evaluated based on: i) static and dynamic stresses obtained in Step I, and ii) laboratory cyclic triaxial test results performed in undrained conditions. Finally, dissipation of pore water pressures during the earthquake is evaluated as a function of time through a finite element solution of the diffusion equation. A numerical example illustrates the actual significance of the dissipation process in the magnitude and distribution of pore water pressures induced by earthquake motions, and safety factors in post-earthquake stability analysis.

## INTRODUCTION

This study, part of the broader subject of behaviour of embankment dams under seismic excitations, is centered on a computational scheme to evaluate generation and dissipation of earthquake-induced pore water pressures.

For a comprehensive review of various aspects of the seismic behaviour of embankment dams the reader is referred to [1], where both analytical procedures and results of the field observations are discussed, providing a conceptual framework for the present study.

In general terms, the methodology used here to predict embankment behaviour follows that developed by Seed and coworkers at the University of California in Berkeley, in aspects ranging from static and dynamic stress analysis to interpretation and correlation with field observations of the results of laboratory cyclic triaxial tests. In contrast to more ambitious developments [2], [3], [4] where general constitutive equations are proposed including the pore water pressure as an explicit variable which is solved for simultaneously with soil displacements and strains, the approach followed here decouples the generation of dynamic pore water pressures from the process of dissipation (or diffusion) due to the relatively high permeability of gravels utilized in embankment shells. Thus, in the foregoing dissipation analysis, the field variable describing the potential for pore water pressure generation in undrained conditions is determined first, and then is taken as input for the final step where dissipation is accounted for through the numerical solution of the diffusion equation. Step I consists of the following substeps:

- I.1 Analysis of static stresses due to construction and filling of the reservoir.
- I.2 Earthquake induced dynamic stresses.
- I.3 Laboratory cyclic triaxial tests.

Pore water pressures are evaluated in Step II in the following order:

- II.1 Pore water pressures induced under the assumption that no drainage or dissipation takes place.
- II.2 Dissipation of pore water pressures simultaneously with the process of generation.

Highlights of main aspects of Step I are briefly discussed in the next three sections, followed by a detailed description of the procedure used to determine the generation and dissipation of pore water pressures. Finally, the analysis of an actual dam design is presented and the implications of various assumptions in the evaluation of post-seismic sliding stability are discussed.

## STATIC ANALYSIS

The static analysis of stress is very important in predicting seismic response of embankment dams since the cyclic strength of gravels used in shells is a function of both normal effective stresses and shear stresses acting before earthquake occurrence. This analysis is usually performed in incremental manner to account for construction

progress and non linear constitutive laws. In the present study, the hyperbolic representation of soil properties was used together with the FEADAM program [5]. After simulating construction stages through a series of loading increments (twelve), another set of loading increments arising from hydrostatic effects due to water impounding is considered. Some difficulties were encountered while simulating the loading stages associated with water impounding. These are caused by the unloading of the upstream shell due to buoyancy, resulting in unrealistic prediction of upward vertical displacements of the crest. This short coming is partly circumvented by introducing hydrostatic effects (both buoyancy and normal pressure in the upstream slope of the impervious core) simultaneously with construction stages. Since FEADAM only handles plane problems, an alternative program may be required in certain cases for 3-D analyses.

#### DYNAMIC STRESSES

Various forms of dynamic stress analysis of embankment dams are currently used. When grouped in terms of their treatment of soil nonlinearities, two general approaches are available: i) Linear equivalent method; and ii) Direct numerical integration of non linear equations. In i) an estimate of dynamic response is found by approximating non linear stress-strain relations through linear ones on the basis of a secant shear modulus, expressed as function of the maximum or effective strain. Damping is also recognized to depend on the soil strain. An iterative procedure is then utilized whereby a series of complete linear analyses are successively performed, each followed by an adjustment of the shear modulus and damping values based on the effective strain of the previous iteration. This general approach has been incorporated into various 1, 2 and 3-D Finite Element Codes like SHAKE [6], LUSH-2 [7], QUAD-4 [8], and others [9]. Since each iteration implies solving a complete linear dynamic problem, both time and frequency domain algorithms can be used. Results of extensive Laboratory research at the University of California in Berkeley characterizing the non linear properties of granular and cohesive soils allows the straight forward application of the linear equivalent method in most practical applications.

It must be recognized however, that the non linear soil characteristics just mentioned do not account for the possibility of pore water pressure increase while shaking progresses. In fact, these properties are derived from steady-state tests with no degradation in time or number of cycles. This is an obvious shortcoming of the decoupled approach, when the dynamic pore water pressures are calculated in terms of the dynamic stresses obtained from an analysis that ignores their potential occurrence. In contrast, its simplicity and success in modeling field observations [1] renders this method of analysis very useful.

Approach ii), accounting for dynamic coupling of strains and pore water pressures has been formulated in [2] and utilized for horizontally layered strata in [3] and [4]. An extensive study with a direct integration scheme is presented in [10].

#### CYCLIC TRIAXIAL TESTS

Cyclic shear strength of soils is usually defined through a series of triaxial tests with different consolidation ratios and confining

pressures. The range of consolidation pressures and deviator stresses are selected for a test program to account for dimensions of the embankment and depth of foundation strata, and for the effective duration of shaking. The effective duration is expressed in terms of the "number of equivalent uniform" cycles that can be associated with the irregular shear stress histograms obtained with the dynamic analysis. This number depends on the particular element chosen for evaluation, and an average value obtained through a set of representative elements is usually adopted. Determination of the number of equivalent cycles is based on Miner's rule for estimating accumulation of damage and is described in detail in [11].

The reader is referred to [12] for interpretation of cyclic tests, leading to the following sets of results:

a) Strength curves

For a given number of equivalent uniform cycles ( $N_{eq}$ ), the cyclic shear strength is expressed as function of the normal static effective stress. Cyclic shear strength curves for  $N=7$  and  $N=20$  are given in Figures 1.a and 2.a for Limay Medio gravels, expressed parametrically in terms of the ratio of static shear stress to the static effective normal stress. The cyclic shear strength is defined as the cyclic shear amplitude required to produce a given axial deformation (in this case 2.5 %) in  $N_{eq}$  cycles.

b) Fatigue curves

They represent the variation of cyclic shear strength for a number of cycles larger than  $N_{eq}$ . Approximated by a straight line in double logarithmic scale, they are indicated in Figures 1.b and 2.b.

c) Pore water pressure curves

The rate of generation of pore water pressure is expressed in terms of the "cycle ratio"  $r_n$ , that is the quotient of the number of cycles  $n$  divided by the number of cycles required to produce a given axial strain (2.5 %). Typical curves for Limay Medio gravels are shown in Figures 3.a and 3.b for different consolidation ratios.

#### GENERATION OF PORE WATER PRESSURES

The procedure followed to evaluate the total increase in pore water pressure under the assumption that no dissipation takes place is described next. Required data from stress analyses for each element in the finite element model is as follows:

- Shear and effective normal static stresses in horizontal planes,  $\tau_{fc}$  and  $\sigma'_{fc}$  respectively.
- Equivalent dynamic shear stress  $\tau_{eq}$ .
- Number of equivalent uniform cycles caused by seismic actions.
- Material cyclic strength  $\tau_c$ , fatigue curves, and curves for the rate of generation of pore water pressures.

FIGURE 1.a CYCLIC STRENGTH CURVE FOR 7 CYCLES ( $\epsilon = 2.5\%$ )  
RELATIVE DENSITY  $D_r = 80\%$

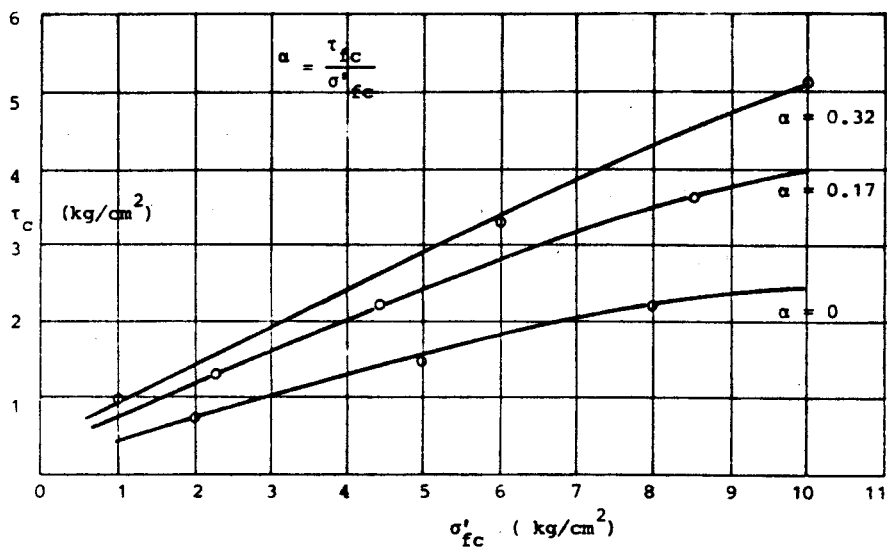


FIGURE 1.b FATIGUE CURVE FOR MORE THAN 7 CYCLES

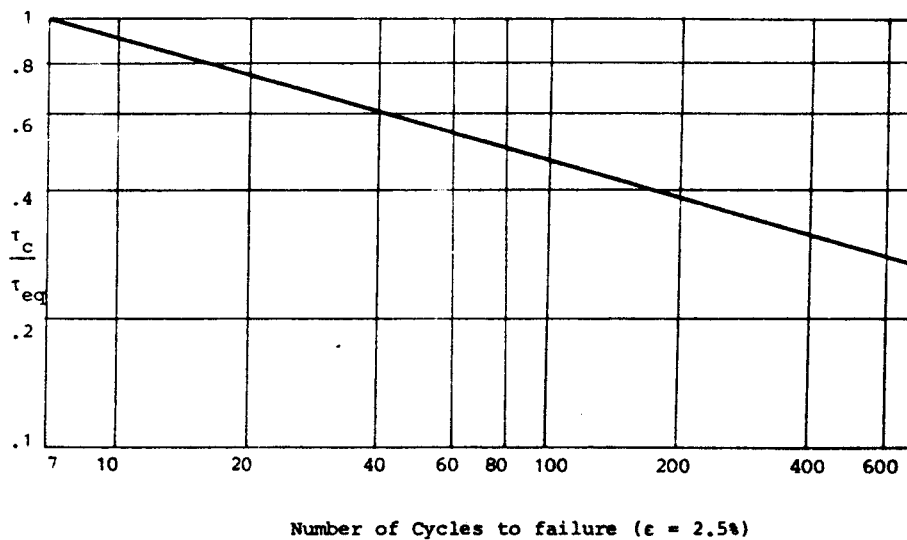


FIGURE 2.a CYCLIC STRENGTH CURVES FOR 20 CYCLES ( $\epsilon = 2.5\%$ )  
RELATIVE DENSITY  $D_r = 80\%$

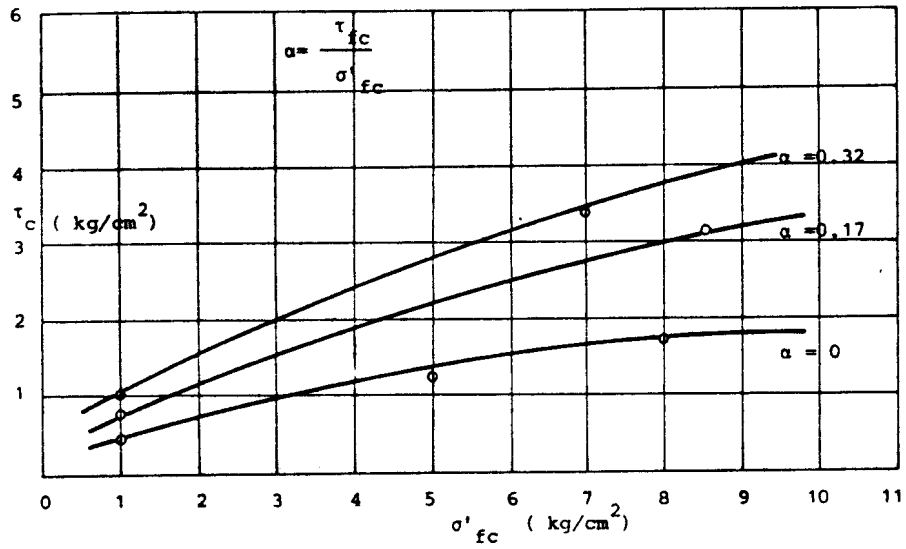


FIGURE 2.b FATIGUE CURVE FOR MORE THAN 20 CYCLES

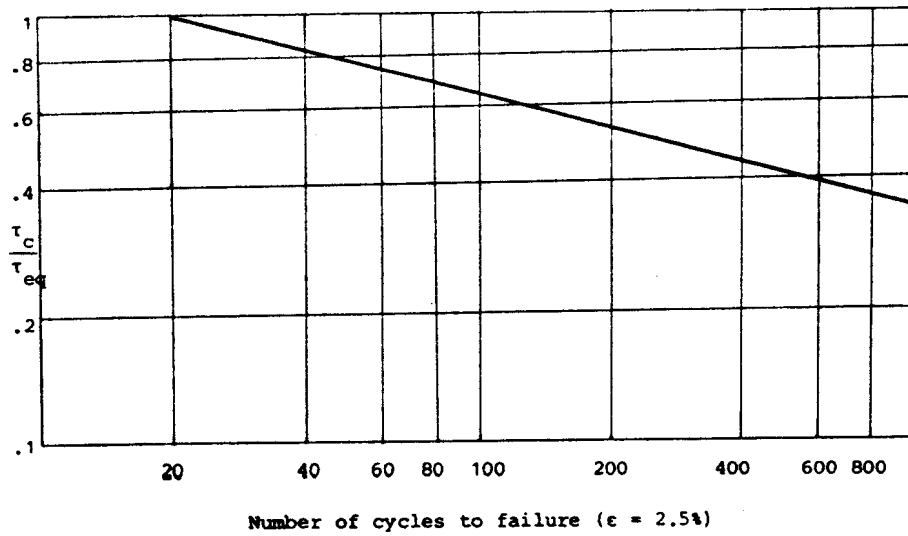


FIGURE 3.a PORE-WATER PRESSURE RATIO  $r_u$

CONSOLIDATION RATIO  $K = \frac{q_u}{\sigma'_3} = 1$

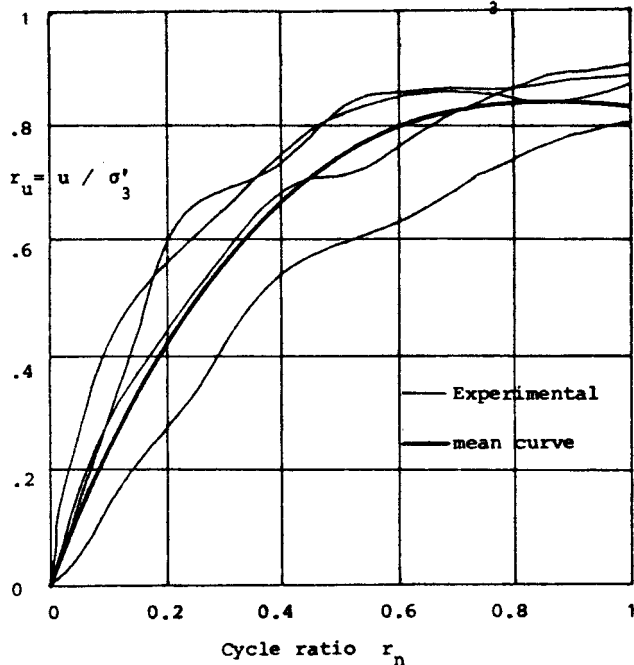
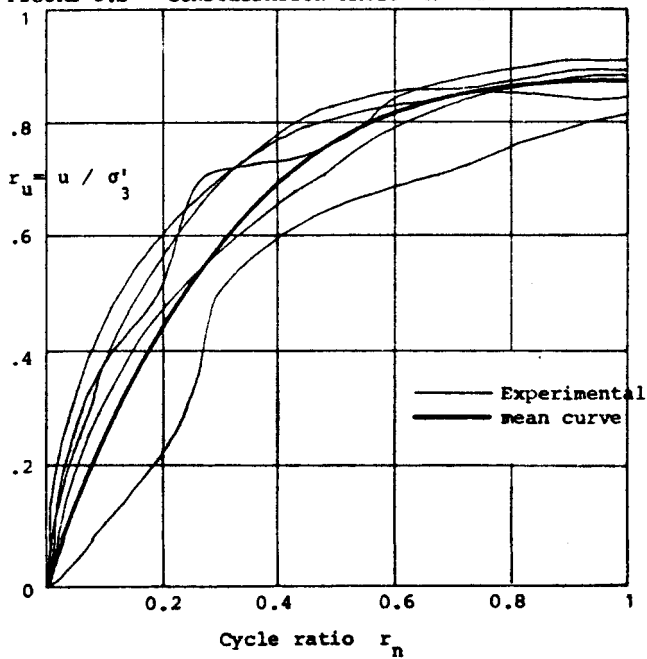


FIGURE 3.b CONSOLIDATION RATIO  $K = 2$



The sequence of calculations to determine pore water pressures depicted in Figure 4 is as follows for each element:

- With the value of the ratio  $\tau_{eq}/\tau_c$ , the number of cycles  $N_1$  required to achieve a given principal strain level or initial liquefaction. This is obtained from the normalized fatigue curve. The ratio of the number of equivalent cycles  $N_{eq}$  to this  $N_1$  is defined as the "cycle ratio"  $r_n$ .
- From pore water pressure generation curves, the pore water pressure ratio  $r_u$  is obtained as function of  $r_n$ ;  $r_u$  is the ratio of pore water pressure increase to confining consolidation pressure. Pore water pressure increases  $\Delta u$  are obtained from  $r_u$  multiplied by the static confining pressure in the element ( $\sigma'_{fc}$ ).

#### DISSIPATION OF PORE WATER PRESSURES

Pore water pressure increases described in the preceding section provide an estimate of values that would occur at the end of the seismic action if there were no dissipation while they are generated. Depending on the magnitude of the seismic event causing the earthquake, the process of pore water pressure increase may take from few seconds to approximately one minute. While this takes place dissipation does occur to some degree possibly leading to their redistribution in shells and foundation. For the purpose of simulation of the dissipation phenomenon, it is assumed that the cycle ratios  $r_n$  achieved at the end of the shaking vary linearly with time during the earthquake. The rate of increase in  $r_n$ , from zero to its maximum value, depends on the estimated duration of the strong phase of ground motions  $T_d$ , and is approximated dividing the final value of  $r_n$  by  $T_d$ . The generated pore water pressure increase  $u_g$  as function of time is thus given by:

$$u_g(t) = \sigma'_{fc} r_u \frac{t}{T_d} \quad (1)$$

where  $r_u$  is the value associated with  $r_n$ .

The diffusion equation that governs distribution of pore pressures is:

$$\frac{1}{m_v \gamma_w} \left[ K_1 \frac{\partial^2 u}{\partial x_1^2} + K_2 \frac{\partial^2 u}{\partial x_2^2} \right] + \frac{\partial u_g}{\partial t} = \frac{\partial u}{\partial t} \quad (2)$$

where  $K_1, K_2$  are permeability coefficients,  $m_v$  is the volumetric compressibility modulus and  $\gamma_w$  the specific weight of water. At free draining surfaces the boundary condition is  $u = 0$ , and at impervious boundaries the normal derivative  $\partial u / \partial n = 0$ . The numerical solution of eq.(2) is performed with an explicit integration in time of a finite element model. Triangular elements with linear variation of  $u$  are utilized. Detailed algebraic expressions for discrete equations are given in Appendix I.

The time integration step  $\Delta t$  must be selected accounting for element mesh size, permeability of the materials and compressibility. With the integration scheme used here it is found necessary to restrict

FIGURE 4 FLOW DIAGRAM FOR DETERMINATION  $r_u$

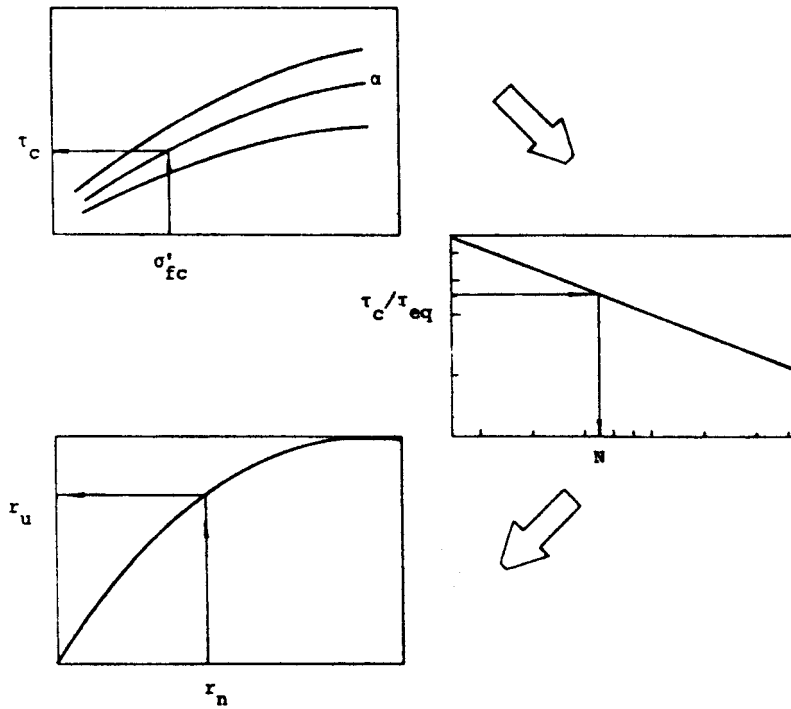
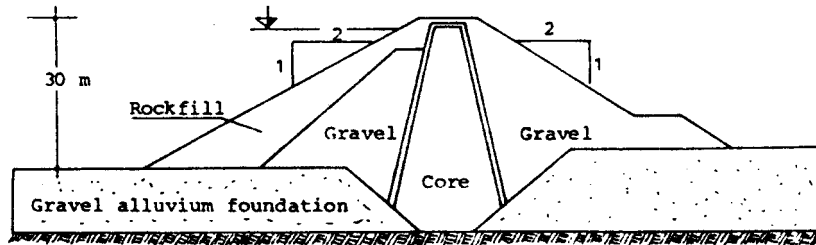


FIGURE 5 CROSS SECTION OF PICHICUN LEUFU DAM



values of  $\Delta t$  according to:

$$\Delta t \leq \frac{h^2 m_v \gamma_w}{4 K} \quad (3)$$

where  $h$  is the minimum mesh size in the same direction where  $K$  represents the permeability coefficient.

At  $t=0$  it is assumed the  $u$  is zero throughout the cross section. Then at any other instant  $t_i$  the value of  $u$  is given by:

$$u(t_i) = u(t_{i-1}) + \dot{u}(t_{i-1}) \Delta t \quad (4)$$

where  $\dot{u}(t_{i-1})$  (rate of change of  $u$  with  $t$ ) is obtained from the discrete form of the left hand terms in eq.(2) that can be explicitly calculated for  $t_{i-1}$ .

#### NUMERICAL EXAMPLE

The Pichi Picún Leufú Dam Project in the Limay River, Argentina, has been selected to illustrate the practical implications of the dissipation of pore-water pressures on the evaluation of the stability of the embankment.

Two different extreme earthquakes have been adopted to assess the seismic performance of the dam. One is a near field earthquake of magnitude  $M_s = 6.5$ , maximum acceleration at rock base of 0.20 g, dominant period of acceleration trace of 0.30 s and duration of 10 seconds, and the other is a far field earthquake of  $M_s = 8$  at a distance of 250 km from the dam, with dominant period of 0.70 s, maximum acceleration of 0.13 g and duration of 60 seconds.

The dam cross section is zoned as indicated in Figure 5. The upstream shell is divided into a rockfill external zone, and a gravel zone with filters in the contact with the impervious core. The foundation alluvium is dense ( $D_r = 80\%$ ) and left in its natural condition.

The static stress analysis was performed with FEADAM program and the dynamic analysis with QUAD 4 program. Results of these analyses are not given in this work for brevity. It may be of interest to indicate that field and laboratory measurements led to estimate the  $(K_2)_{\max}$  [8] value for the alluvium at 100 and 120 for the gravel shells. Since no data were available for the rockfill zone, the same value adopted for gravels was used in evaluating dynamic shear moduli for the QUAD 4 model. From reloading triaxial test  $m_v$  is found to be  $0.001/\sigma'_m$ .

To analyze the dissipation process two different conditions were assumed as representative of limiting cases:

i) Permeability in the vertical direction is zero, hence only horizontal dissipation is allowed to occur. This is considered to include the possibility that segregation of fine materials may lead to very low permeability in the vertical direction.

ii) Permeability in the vertical direction is half of that in the horizontal direction.

Field measurements in the river alluvium have yielded an estimate

of the horizontal permeability coefficient  $K_1 = 10^{-3}$  m/s, which is used in all numerical examples both for the gravel shells and foundation alluvium. In absence of specific information for the rockfill, the same value was conservatively assumed in one case, and a value ten times higher in another case.

Three different cases of 2-D dissipation hypotheses have been considered:

- Case 1. No dissipation takes place in the foundation alluvium within the lapse of time considered in the analysis. This case corresponds to the situation where a very low permeability of the alluvium in the vertical direction is encountered. Boundary conditions of the problem do not allow for significant horizontal drainage in the horizontal direction.
- Case 2. Dissipation takes place both in shells and foundations.
- Case 3. Rockfill permeability is ten times larger than for gravels. No dissipation in the foundation is allowed.

To illustrate further the dissipation process, a horizontal drain at the base of the rockfill has been studied.

An initial evaluation of pore-water pressures generated under the near field earthquake (number of equivalent uniform cycles equal to 7) and the far field (number of equivalent uniform cycles equal to 20) showed that the latter one represents the most severe condition for stability although stresses and accelerations associated with it are lower than those of the former. For this reason dissipation analyses have been performed with the far field earthquake.

Figure 6 contains a mesh pattern used in conjunction with QUAD 4, for which values of generated pore-water pressures assuming no dissipation are indicated for each element.

Figures 7 to 9 contain contour lines of constant pore-water pressure ratios  $r_u$  for cases 1 to 3 after  $t_0$  seconds of the start of shaking. Figure 10 has the same representation for the case of the horizontal drain.

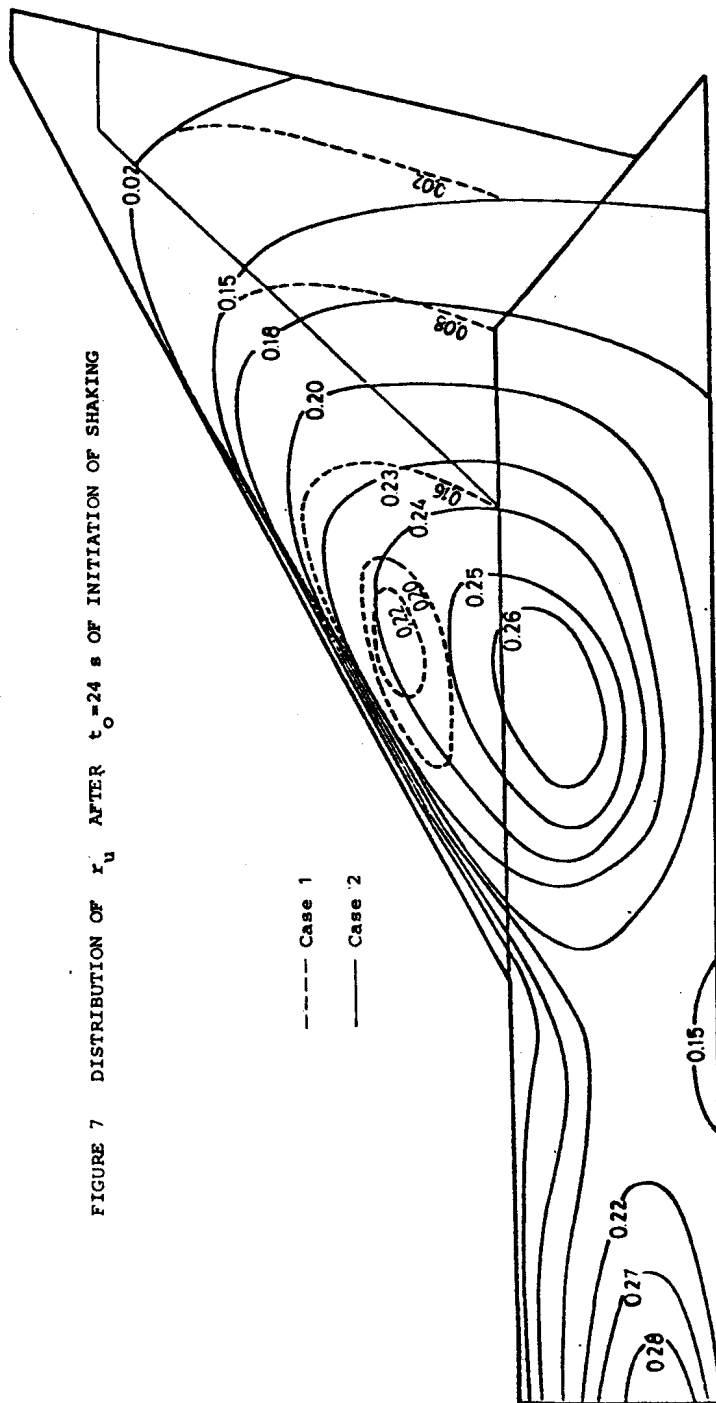
Figures 11 to 13 represent the evolution in time of  $r_u$  for points in the foundation and shell, that illustrate the effect of dissipation in  $r_u$  values.

Table I summarizes the static sliding safety factors at the end of shaking for various cases and assumptions. Three potential circular wedges were analyzed with the simplified Bishop method. From these results the following observations can be made:

- i) Safety factors increase considerably when the dissipation process is included in the analysis. Horizontal dissipation alone produces a considerable increase in calculated safety factors.
- ii) Considering dissipation in the foundation may lead to lower safety factors in wedges that predominantly involve the shells. This suggests that generation of pore-water pressures in the foundation are deleterious both for foundation and shell stability conditions.



FIGURE 7 DISTRIBUTION OF  $k_u$  AFTER  $t = 24$  s OF INITIATION OF SHAKING



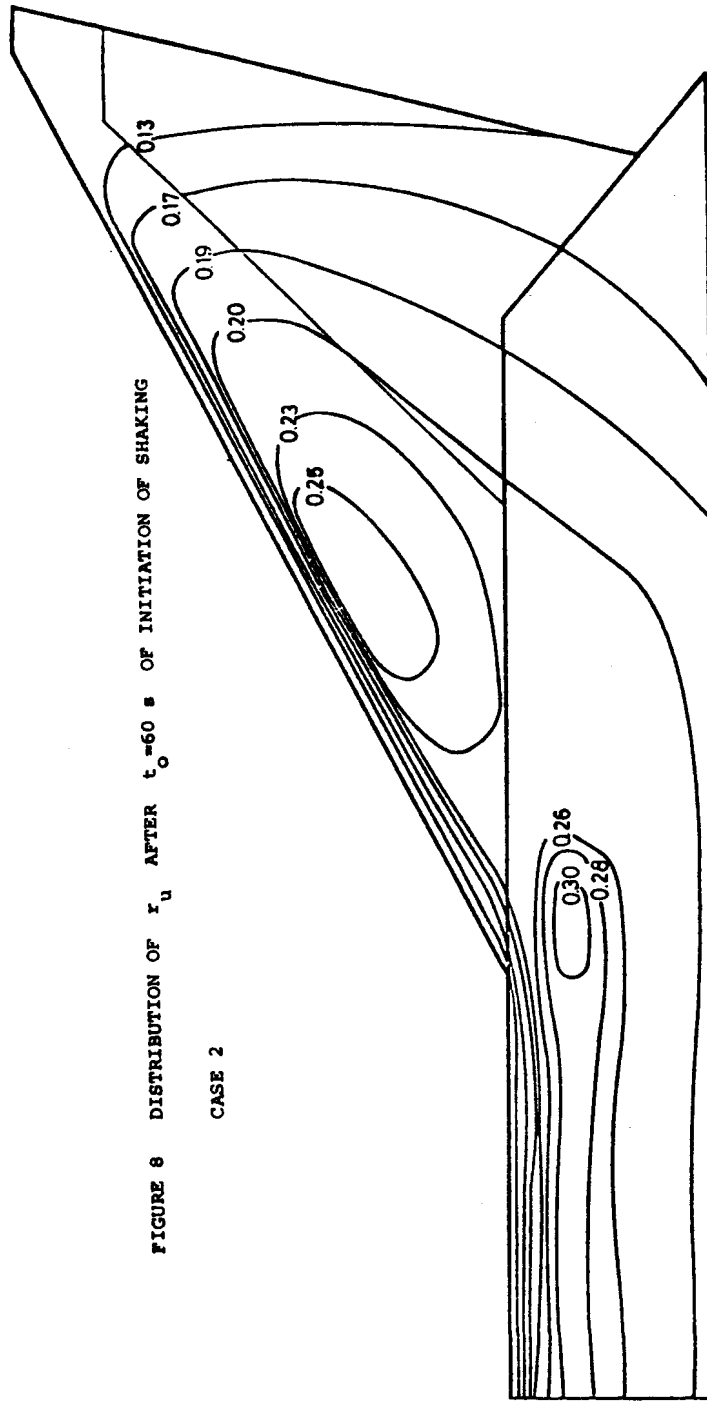
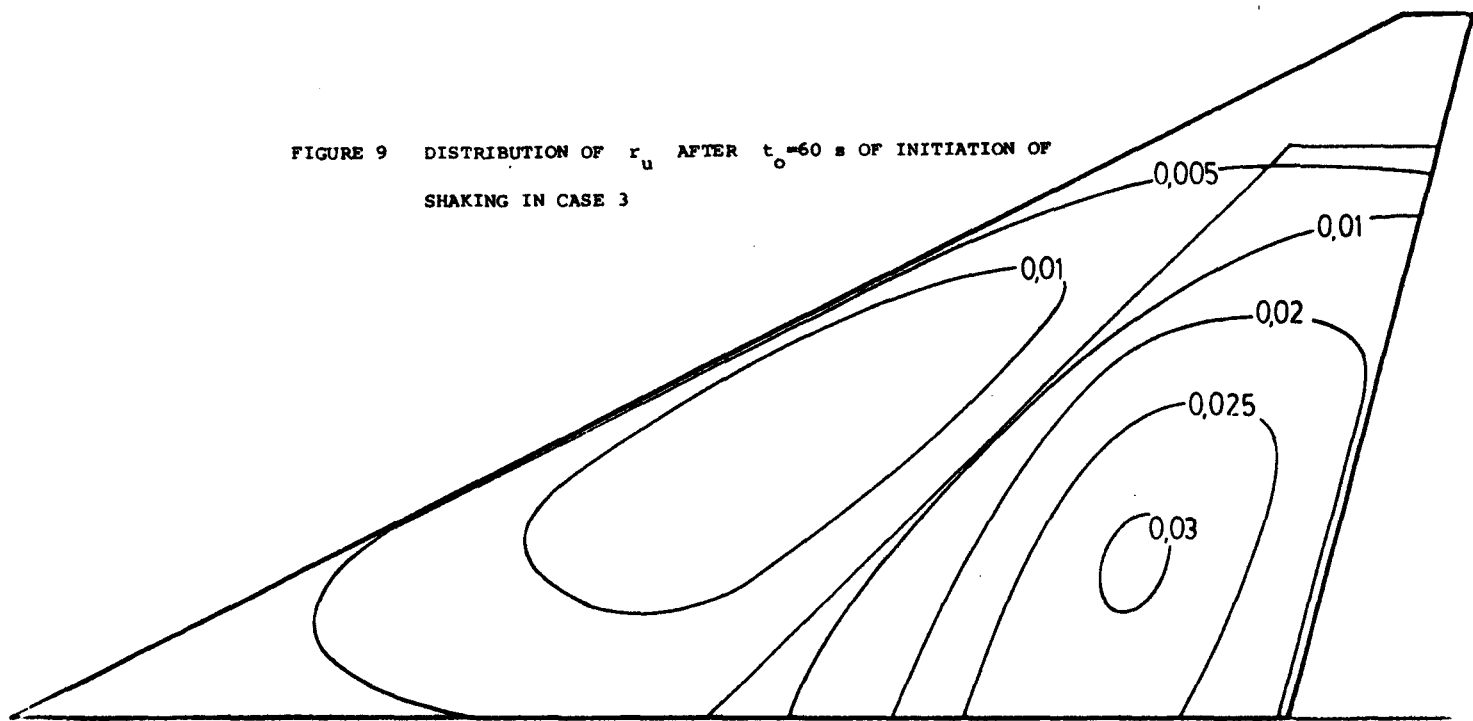


FIGURE 8 DISTRIBUTION OF  $r_u$  AFTER  $t_0 = 60$  s OF INITIATION OF SHAKING

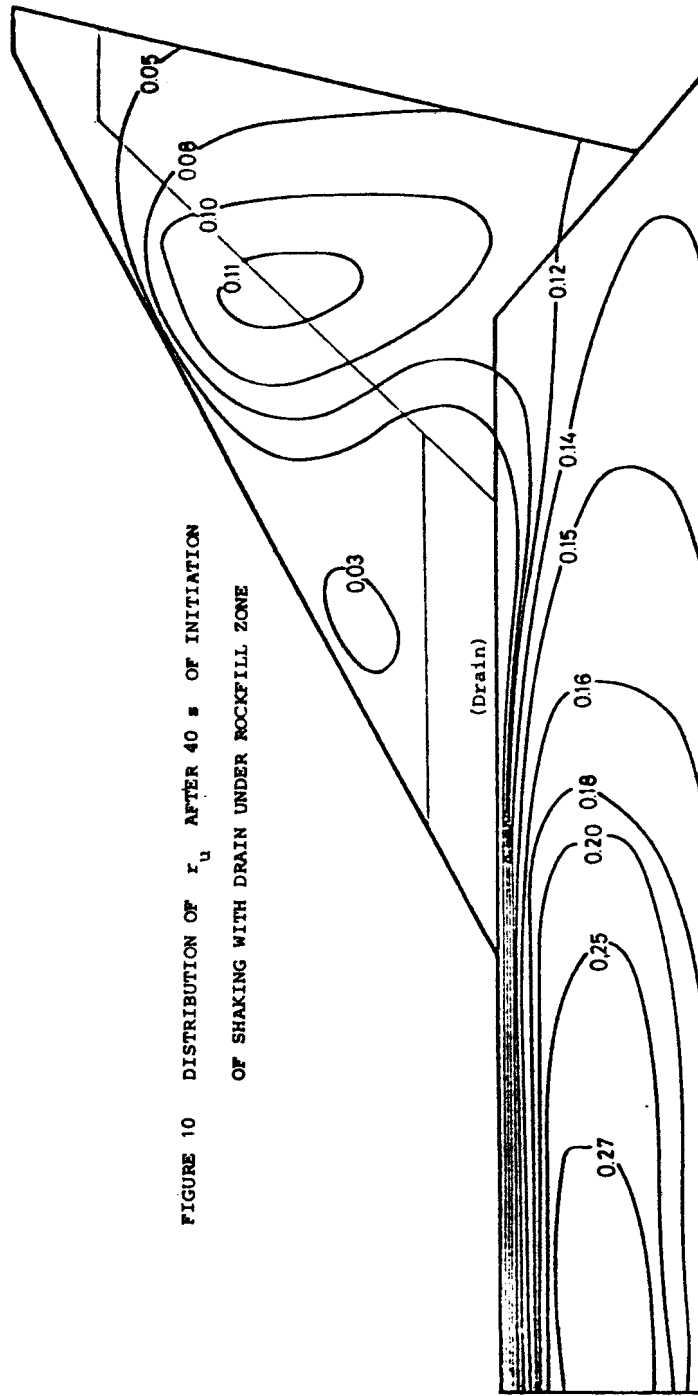
CASE 2

FIGURE 9 DISTRIBUTION OF  $r_u$  AFTER  $t_o = 60$  s OF INITIATION OF SHAKING IN CASE 3



Foundation alluvium not represented in the figure.

FIGURE 10 DISTRIBUTION OF  $r_u$  AFTER 40 s OF INITIATION  
OF SHAKING WITH DRAIN UNDER ROCKFILL ZONE



$$r_u = u / \sigma_{3c}^i$$

FIGURE 11 EVOLUTION OF  $r_u$  FOR A POINT IN THE FOUNDATION

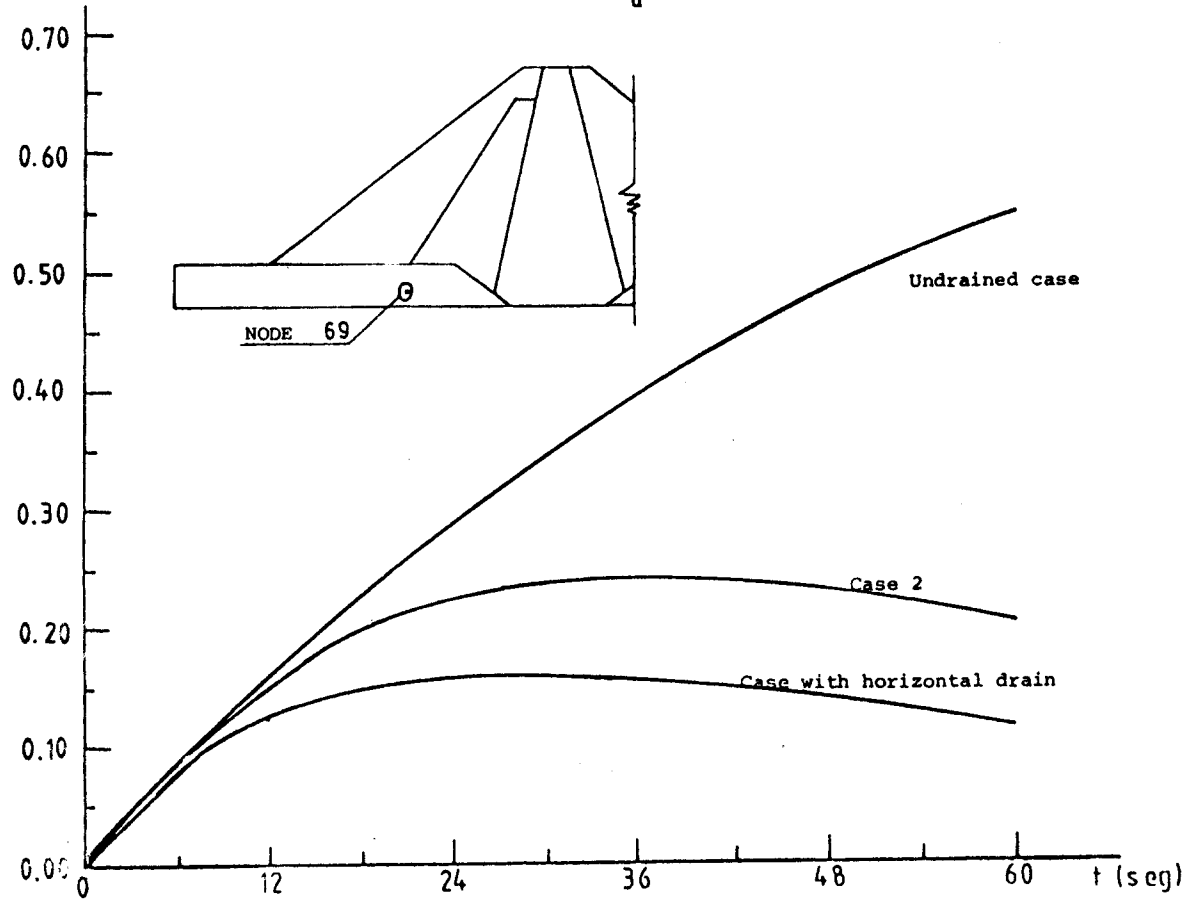


FIGURE 12 EVOLUTION OF  $r_u$  FOR A POINT AT BOUNDARY OF ROCKFILL ZONE

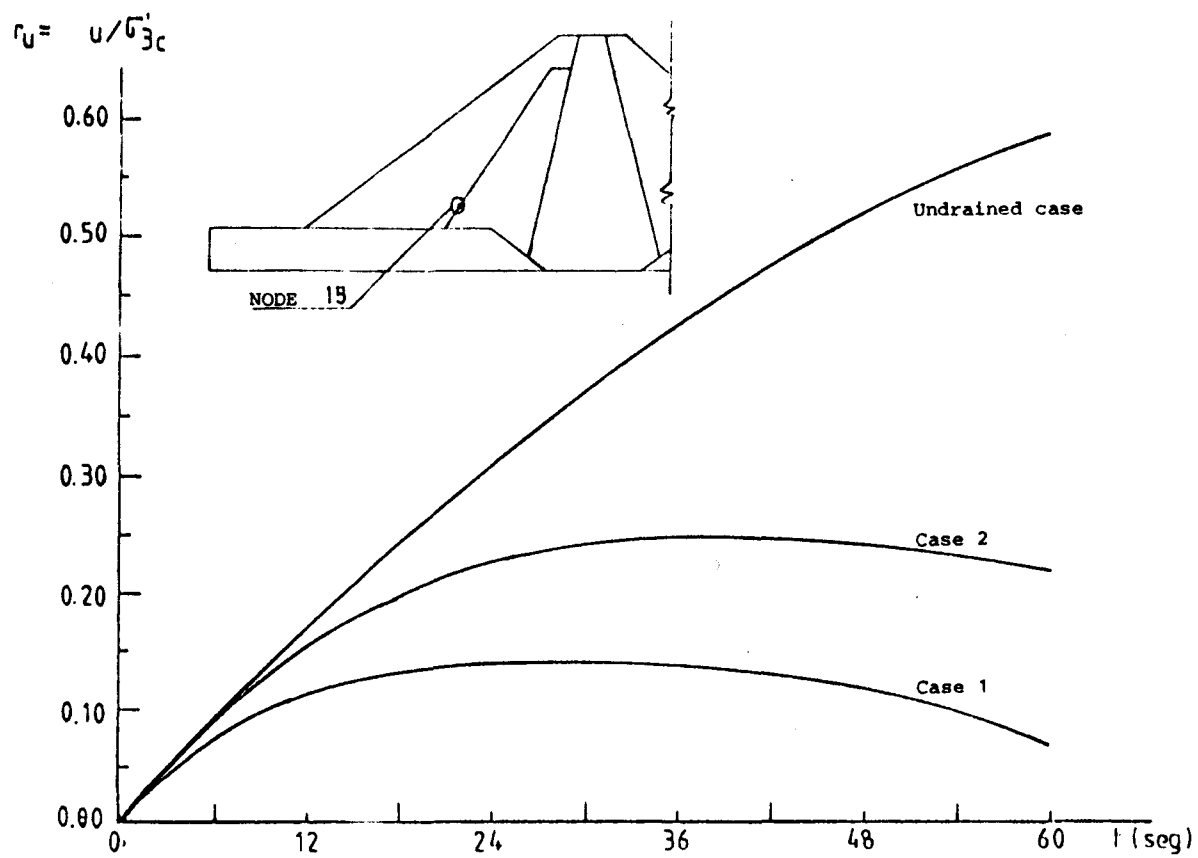


FIGURE 13 EVOLUTION OF  $r_u$  FOR A POINT IN ROCKFILL ZONE

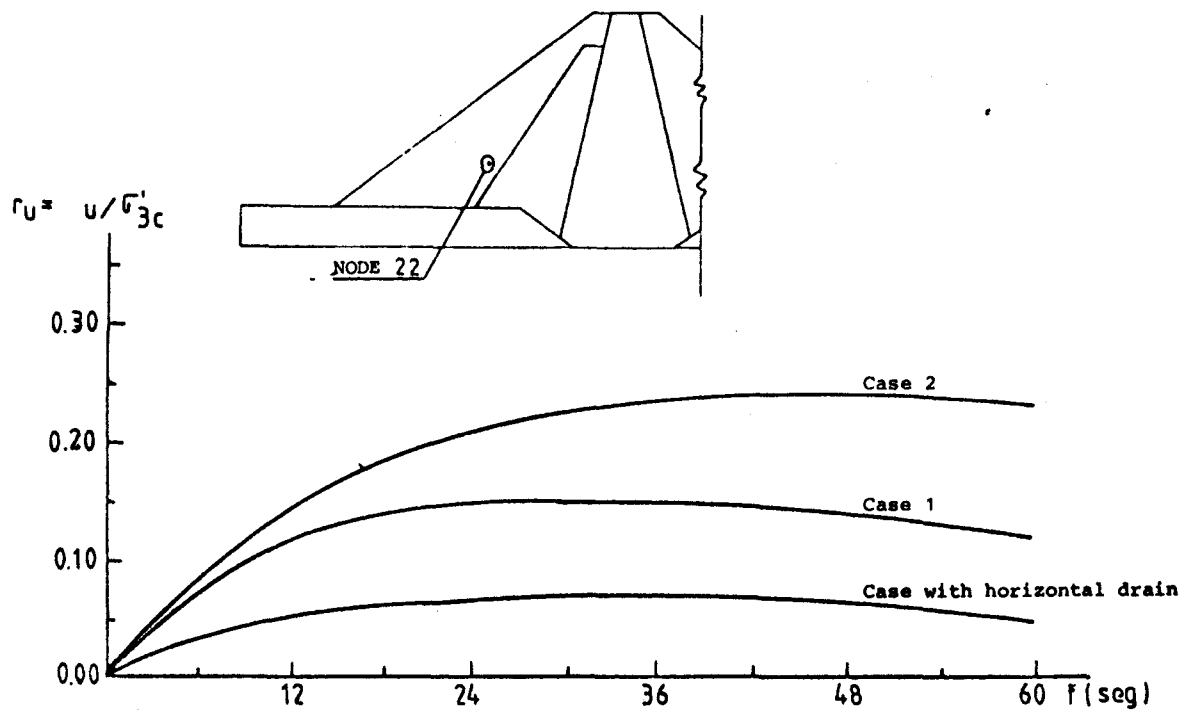
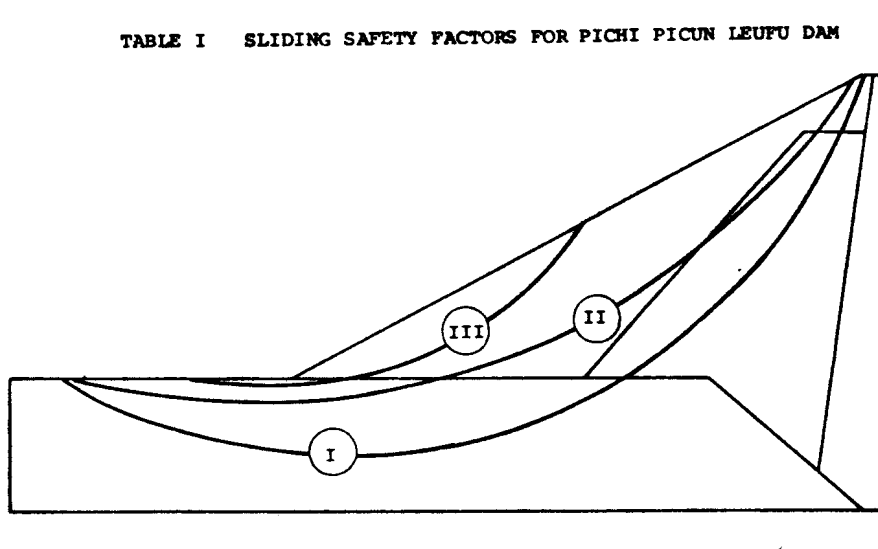


TABLE I SLIDING SAFETY FACTORS FOR PICHU PICUN LEUFU DAM



WEDGE	UNDRAINED		1-D Dissip.	2-D Dissipation		
				Case 1	Case 2	Case 3
	Near F.E.	Far F.F.	Far F.E.	Far Field Earthquake		
I	1.72	1.20	1.67	1.68	1.97	1.75
II	1.48	1.24	2.00	2.07	1.83	2.28
III	1.83	1.64	1.83	2.08	1.80	2.28

### CONCLUSIONS

A decoupled finite element analysis of dissipation of pore-water pressures arising from dynamic excitation of gravel shell embankment dams has been presented. A practical numerical example has shown that this phenomenon bears significantly on the assessment of stability under seismic excitations.

### ACKNOWLEDGEMENT

The writers express their appreciation to Professor Arnoldo J.L. Bolognesi for introducing them into various aspects of soil mechanics involved in this work. Also to Inconas Consulting Engineers for utilizing experimental data developed for the Limay Medio Hydroelectric Projects under contract with Hidronor S.A. of Argentina.

### REFERENCES

- 1 Seed, H.B., " Considerations in the Earthquake Resistant Design of Earth and Rockfill Dams" , Geotechnique 29, N°3, 1979, pp. 215-263.
- 2 Ghaboussi, J., Wilson, E.L., " Variational Formulation of Dynamics of Fluid Saturated Porous Elastic Solids ", J. Engng. Mech. Div., ASCE, Vol.98, EM 4, August 1972, pp. 947-963.
- 3 Ghaboussi, J., Dikmen, U., " Liquefaction Analysis of Horizontally Layered Sands ", J. Geotech. Engng. Div., ASCE, Vol. 104, GT 3, March 1978, pp.341-356.
- 4 Ghaboussi, J., Dikmen, U., " Liquefaction Analysis of Multidirectional Shaking ", J. Geotech. Div., ASCE, Vol. 107, GT 5, May 1981, pp. 605-627.
- 5 Duncan, J., Wong, K., Ozawa, " FEADAM: A Computer Program For Finite Element Analysis of Dams ", Report UCB/GT/80-02, December 1980.
- 6 Schnabel, B., Lysmer, J., Seed, H.B., " SHAKE: A Computer Program for Earthquake Response Analysis of Horizontally Layered Sites ", EERC Report EERC 72-12, University of California, Berkeley, December 1972.
- 7 Lysmer, J., Udaka, T., Seed, H.B., Hwang, R., " LUSH-2: A Computer Program For Complex Response Analysis of Soil Structure Systems ", EERC Report EERC 74-4, University of California, Berkeley, April 1974.
- 8 Idriss, I.M., Lysmer, J., Hwang, R., Seed, H.B., " QUAD 4: A Computer Program for Evaluating the Seismic Response of Soil Structures by Variable Damping Finite Element Procedures ", EERC Report EERC 73-16, University of California, Berkeley, May 1973.
- 9 Mejia, L.H., Seed, H.B., Lysmer, J., " Dynamic Analysis of Earth Dams in Three Dimensions ", J. Geotech. Div., ASCE, Vol. 111, GT 12, December 1982, pp. 1586-1604.
- 10 Prévost, J., Abdel-Ghaffar, M., Elgarni, M., " Nonlinear Hysteretic Dynamic Response of Soil Systems ", J. Engng. Mech. Div., ASCE, Vol. 111, EM 5, May 1985, pp. 696-713.

- 11 Annaki, M., Lee, K., "Equivalent Uniform Cycle Concept for Soil Dynamics ", J. Geotech. Div., ASCE, Vol. 103, GT 6, June 1977, pp. 549-564.
- 12 Banerjee, N., Seed, H., Chan, C., "Cyclic Behaviour of Dense Coarse-Grained Materials in Relation to the Seismic Stability of Dams " EERC Report EERC 79-13, University of California, Berkeley, June 1979.

#### APPENDIX I . DISCRETIZED FORM OF DIFFUSION EQUATION

For a linear variation of  $u$  between nodes of a mesh of triangular elements, the discrete form of eq.(2) to determine the unknown vector  $[u]_m$  at instant  $t=t_m$  can be expressed as follows:

$$[R]_{m-1} = [D] [u]_{m-1} + [R_g]_{m-1} \quad (\text{equation at } t=t_{m-1})$$

where:  $[R]_{m-1}$  Vector of rates of change of  $u$  at  $t=t_{m-1}$

$[D]$  Matrix of diffusion coefficients given below

$[u]_{m-1}$  Vector of known  $u$ 's at  $t=t_{m-1}$

$[R_g]_{m-1}$  Vector of rates of  $u_g$  at instant  $t=t_{m-1}$

together with:  $[u]_m = [u]_{m-1} + [R]_{m-1} \Delta t$

The explicit form of matrix  $[D]$  is:

$$D_{ij} = \sum_{n=1}^M \left[ 1/(4 A^2 m_v \gamma_w) (K_1 a_2^i a_2^j + K_2 a_1^i a_1^j) \right]_n$$

where  $A$  is the area of the element considered in the summation over  $n$  elements connecting nodes  $i$  and  $j$ .

$a_s^i$  is the oriented element side of node  $i$  (counterclockwise direction) projected in the  $x_s$  coordinate direction.

$M$  is the limit of summation, that varies as follows:

for  $i=j$ ,  $M$  refers to all elements surrounding node  $i$ .

for  $i \neq j$ ,  $M$  refers to all elements connecting nodes  $i$  and